



Wide spectrum solar energy harvesting through an integrated photovoltaic and thermoelectric system



Yongliang Li^{a,*}, Sanjeeva Witharana^a, Hui Cao^a, Mathieu Lasfargues^a, Yun Huang^b, Yulong Ding^{a,b,c}

^a Institute of Particle Science and Engineering, University of Leeds, Leeds LS2 9JT, UK

^b Institute of Process Engineering, Chinese Academy of Sciences, Beijing 100190, China

^c School of Chemical Engineering, University of Birmingham, Edgbaston, Birmingham B15 2TT, UK

ARTICLE INFO

Article history:

Received 3 January 2013

Received in revised form 29 July 2013

Accepted 12 August 2013

Keywords:

Solar power

Photovoltaic panel

Spectrum beam splitting

Thermoelectric generator

Energy storage

ABSTRACT

This paper proposes a power system concept that integrates photovoltaic (PV) and thermoelectric (TE) technologies to harvest solar energy from a wide spectral range. By introduction of the 'spectrum beam splitting' technique, short wavelength solar radiation is converted directly into electricity in the PV cells, while the long wavelength segment of the spectrum is used to produce moderate to high temperature thermal energy, which then generates electricity in the TE device. To overcome the intermittent nature of solar radiation, the system is also coupled to a thermal energy storage unit. A systematic analysis of the integrated system is carried out, encompassing the system configuration, material properties, thermal management, and energy storage aspects. We have also attempted to optimize the integrated system. The results indicate that the system configuration and optimization are the most important factors for high overall efficiency.

© 2013 Published by Elsevier B.V. on behalf of Chinese Society of Particuology and Institute of Process Engineering, Chinese Academy of Sciences.

1. Introduction

We are living in an era where energy security faces multiple threats; the oil spike is signaling an end to energy security, while geo-political instabilities are pushing even the most powerful nations to search for local energy solutions. One obvious consequence of this change is the global drive toward renewable energy options. The European Union and China plan to harvest 20% and 15%, respectively, of their total power generation from renewable energy sources by 2020. As a renewable energy source, the Sun is the oldest and most potent source of energy and life known to humanity. Human civilization has been tied to the Sun so closely that the Sun was revered as a God long before the discovery of photocatalysis in plants. The Sun delivers 1.2×10^5 TW of solar radiation to the Earth, which is three orders of magnitude higher than the current total energy consumption on the planet (Crabtree & Lewis, 2007; Thirugnanasambandam, Iniyan, & Goic, 2010). Solar power is artificially extracted in the forms of electricity (solar photovoltaic, PV) and heat (solar thermal). Solar PV panels are the most straightforward way to convert solar radiation

into high-grade electricity, but the theoretical upper limit of the conversion efficiency of these panels is estimated to be around 30% (Beard & Ellingson, 2008; Nozik, 2001; Odeh & Behnia, 2009; Yang & Yin, 2011). In practice, the efficiency depends on a variety of factors, and is typically approximately 40–50% below the theoretical maximum (Royne, Dey, & Mills, 2005).

This low conversion efficiency has become a major problem in solar cell science and engineering, and has made it impossible to capture energy from across the wide solar spectrum with a single semiconductor material (Vorobiev, González-Hernández, Vorobiev, & Bulat, 2006). Although the use of combinations of different and specialized materials with intermediate band gaps has been proposed to overcome this problem (Henry, 1980; Luque & Martí, 2001), these materials are expensive. An alternative option is the integration of PV cells with a heat-to-electricity energy converter in the form of a thermoelectric (TE) generator, which can directly convert thermal energy into electricity. Despite the comprehensive attention that PV–TE hybrid systems have gained in the recent past (Kraemer et al., 2008; Miljkovic & Wang, 2011; Rockendorf, Sillmann, Podlowski, & Litzenburger, 1999; Vorobiev et al., 2006; Yang & Yin, 2011), the low conversion efficiency of the TE modules based on current materials and the elevated PV operating temperature, which reduces the cell efficiency, remain major obstacles to the development of these systems. In addition, the

* Corresponding author. Tel.: +44 01133432543.

E-mail addresses: y.li@leeds.ac.uk, yongliang.li@hotmail.co.uk (Y. Li).

presence of TE devices in the market is fairly limited because of their low ‘figure of merit’ (ZT). For instance, bismuth telluride (Bi_2Te_3), which is the preferred TE material in the current PV–TE hybrids, has $ZT \sim 1$ (Omer & Infield, 1998; Rowe, 1995; Tritt, Böttner, & Chen, 2008). Yang and Yin (2011) showed through their experiments that there was literally no difference in electric power output between a water-cooled PV system and a PV–TE-hot water system. Van Sark (2011) argued that for PV–TE hybrid systems to become economically viable, the conversion efficiency of the TE module must increase by a minimum of 10 times that of the present efficiency. Therefore, what is really needed to make these systems viable is a breakthrough in TE materials development. Although quantum well and quantum dot techniques promise to produce highly efficient and cost effective TE materials (Kovalenko et al., 2010; Nolas, Sharp, & Goldsmid, 2001; Scheele et al., 2009), these materials may not reach the market in the foreseeable future. With regard to the issue of reducing the PV operating temperature, attention has been drawn to a solar spectrum splitting system in which the PV cells and the thermal processes run in parallel (Kraemer et al., 2008). A spectral beam splitter would only allow the short wavelength solar spectrum to reach the PV receiver, thus substantially reducing both the heat load and the operating temperature of the cell (Imenes & Mills, 2004).

However, matching the Sun’s diurnal power supply with the time-dependent power demand remains a major challenge for solar-to-electricity systems (Li, Zhu, Cao, Sui, & Hu, 2009; Maclay, Brouwer, & Samuelsen, 2007). Although this problem can be solved by exchanging power with the electricity grid, the addition of certain energy storage devices to the PV systems is desirable to reduce the load change on the grid and even provide power-on-demand via a stand-alone PV system. The conventional lead–acid battery is still the most common energy storage device, while thermal energy storage is emerging as a promising alternative option. Recently, greater focus has been placed on high-grade cold storage technology, which enables high performance recovery of solar thermal energy (Li, Chen, & Ding, 2010; Li, Jin, Chen, Tan, & Ding, 2011).

In this paper, we propose a spectral beam splitting based PV–TE hybrid power system with an integrated high-grade cold storage device. The PV cell and the TE generator can operate either separately or synchronously, depending on the power demand. At off-peak times, the ambient resources supply the cooling load of the system, and the excess electricity is stored in the form of high-grade cold in a deep freezer. At peak times, the stored cold is used to supercool both the PV cell and the TE generator to increase their power output. This integration scheme would enable the system to deliver power at the desired times and rates.

2. Description of the integrated system

PV cells are one of the most promising technologies for conversion of incident solar radiation into electric power. However, this technology is still far from being able to compete with fossil fuel-based energy conversion technologies because of its relatively low efficiency and energy density. Theoretically, there are three unavoidable losses that limit the solar conversion efficiency of a device with a single absorption threshold or band gap E_g : (1) *incomplete absorption*, where photons with energies below E_g are not absorbed; (2) *thermalization* or *carrier cooling*, where solar photons with sufficient energy generate electron–hole pairs and then immediately lose almost all energy in excess of E_g in the form of heat; and (3) *radiative recombination*, where a small fraction of the excited states radioactively recombine with the ground state at the maximum power output (Hanna & Nozik, 2006; Henry, 1980). Taking an air mass of 1.5 as an example, for different band gap E_g these

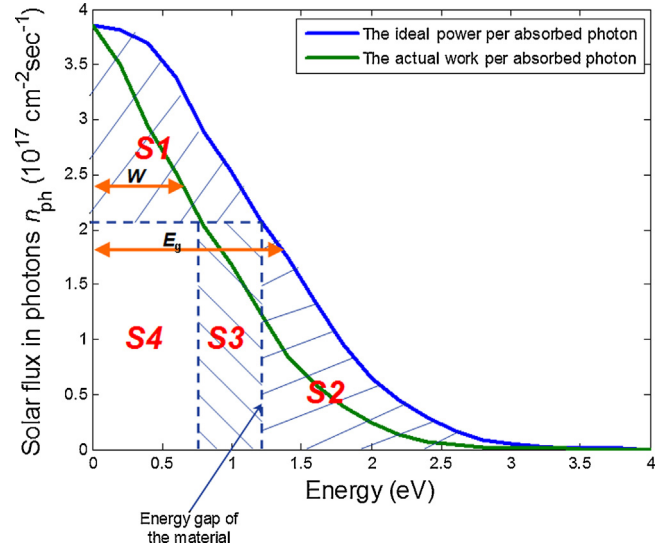


Fig. 1. Graphical analysis of the efficiency of a single band gap PV cell (Henry, 1980).

three losses can be calculated and the results are indicated by areas S1, S2, and S3 in Fig. 1. Note that the area under the outer curve is the solar power per unit area, and that only S4 can be delivered to the load.

In Fig. 1 the actual work per absorbed photon W is related to the operating temperature and the concentration ratio, and is calculated using the following equations (Henry, 1980):

$$W \cong E_g - \kappa T \left[\ln\left(\frac{A}{en_{ph}C}\right) + \ln\left(1 + \frac{eV_m}{\kappa T}\right) + 1 \right], \quad (1)$$

$$A = \frac{2\pi e(n^2 + 1)E_g^2 \kappa T}{h^3 c^2}. \quad (2)$$

Here, κ , e , h , and c are the Boltzmann constant, an electron charge, the Planck constant, and the speed of light, respectively. T , C , and n_{ph} are the operating temperature, the concentration ratio (defined as the average solar flux through the receiver divided by the ambient direct normal solar radiation), and the solar flux in photons, respectively. n is a constant related to the radiation angles that can be assigned a value of 3.6. The voltage at the maximum power point eV_m is governed by the equation shown below:

$$eV_m = E_g - \kappa T \left[\ln\left(\frac{A}{en_{ph}C}\right) + \ln\left(1 + \frac{eV_m}{\kappa T}\right) \right]. \quad (3)$$

Fig. 1 shows that a decrease in the radiative recombination loss can be seen within the PV cell when the distance between the outer curve and the inner curve is reduced. The influence of operating temperature of the PV cell can also be examined using the above approaches and the results are shown in Fig. 2, which indicates that a decrease in the operating temperature would enhance the efficiency of the PV cell. As a result cooling and even supercooling of the cell play an important role on its performance. Areas S4 in Figs. 1 and 2 show that the best band gap at the maximum power point may vary, depending on the operating temperature.

Similarly the effect of the concentration ratio on the cell performance is shown in Fig. 3. The concentration ratio has a much smaller effect on the efficiency of the PV than the temperature. More importantly, the concentrating devices may offer cost benefits by reducing the PV area required to convert a specific amount of solar power (Imenes & Mills, 2004). However, it should be noted that an increase in the concentration ratio is accompanied by a

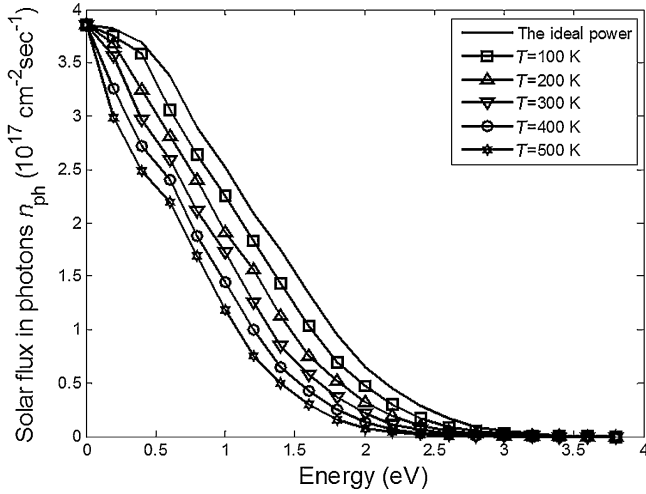


Fig. 2. Effect of the operating temperatures of the PV cell ($C = 1$) on cell performance.

potential increase in the PV cell temperature or the cooling load per unit cell area, which are both undesirable.

As mentioned earlier, photons with energies lower than E_g are not absorbed by the PV cell. This proportion of the total energy is quite large, especially for semiconductor materials with relatively wide band gaps (accounting for approximately 50% of the solar radiation in the case of a semiconductor with $E_g = 1.75$ eV). Removing this portion of the radiation from the PV cell via spectral beam splitting technology could not only reduce the cooling load, but could also enable energy recovery in the form of high grade thermal energy.

TE generators for thermal energy recovery operate silently and have simple structures with no moving parts (Chen, 1996). They are as reliable as PV panels, and could work for 10 to as much as 30 years on average without any major technical problems (Vorobiev et al., 2006).

The ideal efficiency of the TE generator is dependent on the hot side temperature T_h , the cold side temperature T_c , the dimensionless thermoelectric coefficient ZT (a dimensionless figure of

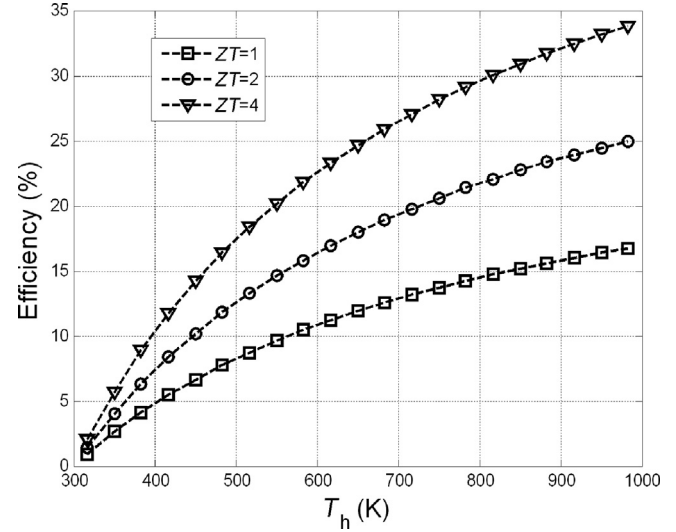


Fig. 4. Effect of the hot side temperature on the ideal efficiency of the TE generator at $T_c = 300$ K and different values of ZT .

merit) of the TE material, and the average operating temperature ($T = (T_c + T_h)/2$), according to the equation below:

$$\eta = \left(1 - \frac{T_c}{T_h}\right) \frac{\sqrt{1+ZT} - 1}{\sqrt{1+ZT} + \frac{T_c}{T_h}}. \quad (4)$$

The figure of merit (Z) is defined as:

$$Z = \frac{S^2 \sigma}{k}, \quad (5)$$

where S , σ , and k are material properties, i.e., the Seebeck coefficient, the electrical conductivity, and the thermal conductivity, respectively. The value of ZT could be estimated reasonably well by using the following values in the calculations: $ZT = 1$ for modern industrial thermoelectrics, $ZT = 2$ for thermoelectrics produced in laboratories (nano-scale microstructures), and $ZT = 4$ for thermionic converters with quantum tunneling (Vorobiev et al., 2006).

The effects of the hot side temperature and the cold side temperature in an ideal TE generator are shown in Figs. 4 and 5,

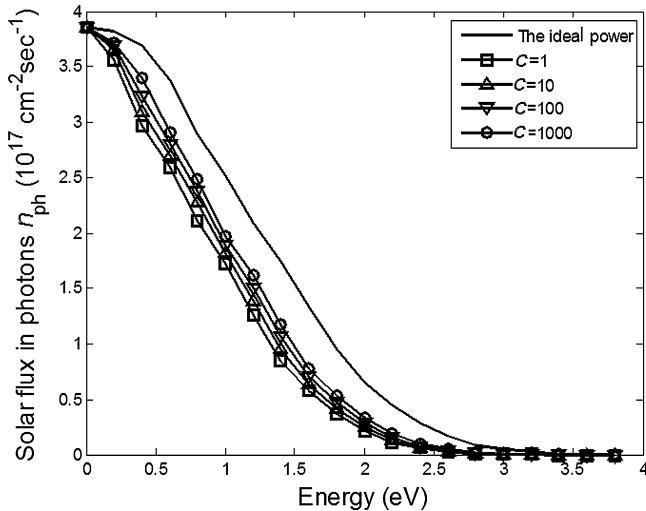


Fig. 3. Effect of the concentration ratios of the PV cell ($T = 300$ K) on cell performance.

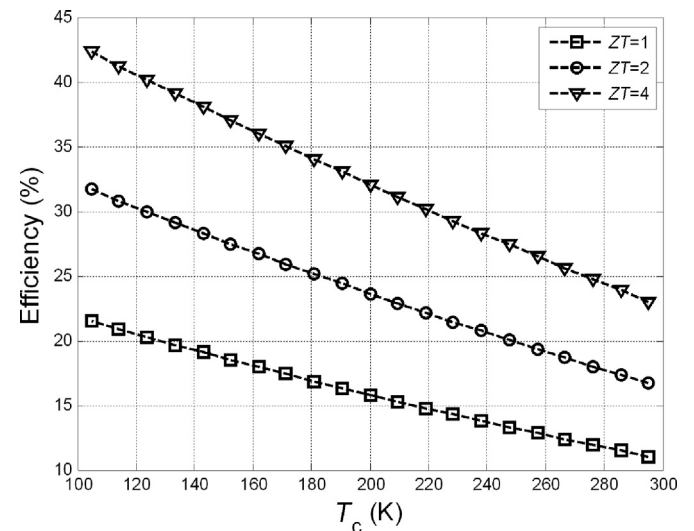


Fig. 5. Effect of the cold side temperature on the ideal efficiency of the TE generator at $T_h = 600$ K and different values of ZT .

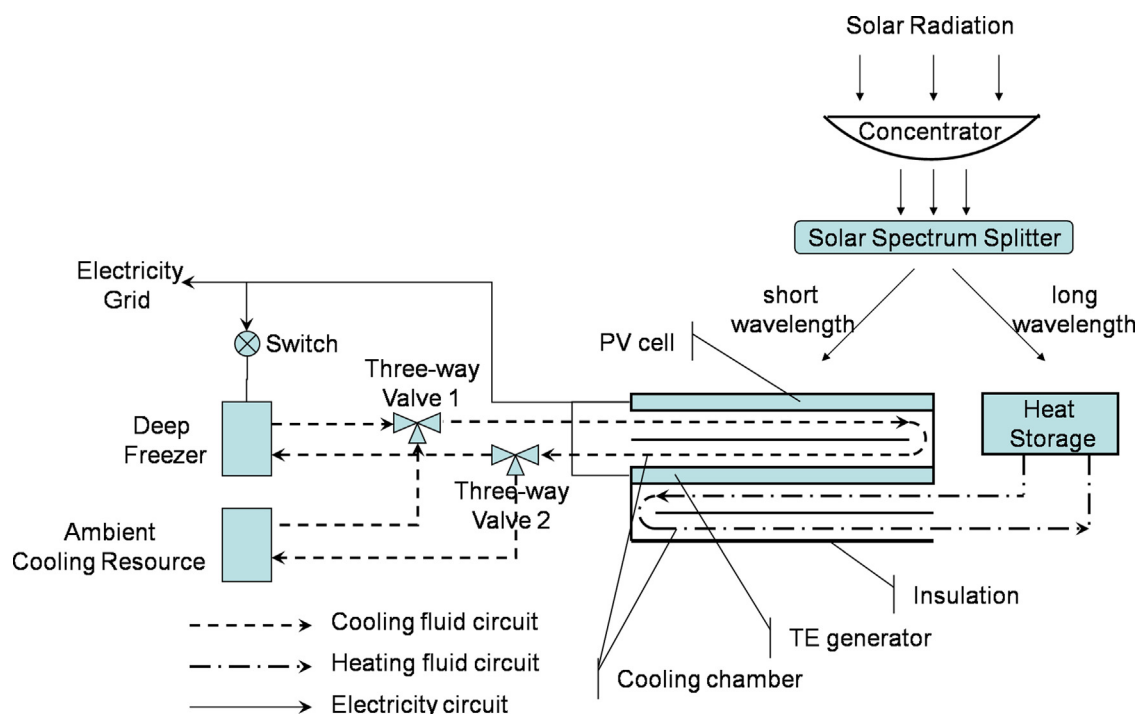


Fig. 6. Schematic of the PV-TE hybrid power system.

respectively. Increasing the hot side temperature and lowering the cold side temperature could improve the TE generator performance. However, lowering the cold side temperature seems to be more prominent when considering TE generators with lower ZT values.

Based on our proposed 'spectrum beam splitting' and thermal energy storage schemes, the PV-TE integrated system is proposed and illustrated in Fig. 6. The system is a combination of a PV cell and a TE generator designed to generate electricity. In contrast to the earlier direct-contact back-to-back structures (Van Sark, 2011), the PV cell and the TE generator in the proposed system are constructed separately on the two sides of a cooling chamber. This novel configuration enables a lower PV operating temperature and a lower TE cold side temperature. The concentrated solar radiation is split by the solar spectrum splitter, with the short wavelength portion directed to the PV cell and the long wavelength portion sent to produce moderate to high temperature thermal energy. The thermal energy stored in the heat storage medium is used to supply the hot side with energy for the TE generator. The cooling chamber can be cooled either by ambient air or by other cold sources, using a low freezing point liquid as the circulating fluid. At off-peak times, ambient air is used to cool the circulating fluid in an external

heat exchanger, and the excess electricity is used to power a deep freezer to generate high-grade cold. The stored cold is then used to supercool the circulating fluid at peak times to increase the power output by reducing the operating temperatures of both the PV cell and the cold side of the TE generator.

Because both the PV cell and the TE generator require stable operating temperatures, it would be efficient to store the thermal energy (for both heating and cooling reservoirs) in phase change materials (PCMs). Inorganic eutectic salt mixtures are strong candidates for thermal energy storage at moderate to high temperatures. These materials are shown in Table 1. For high-grade cold storage, eutectic solutions should be considered. PCM eutectic solutions are mixtures of two or more chemicals, which, when mixed in a particular ratio, have a freezing/melting point that is below the freezing temperature of water, and could offer thermal energy storage facilities down to 159 K. Table 2 provides a list of such materials.

3. System performance and sensitivity analysis

The total conversion efficiency of the hybrid system can be defined as:

$$\eta_{\text{total}} = \alpha_{\text{PV}} \eta_{\text{PV}} + \alpha_{\text{TE}} \eta_{\text{IA}} \eta_{\text{TE}}. \quad (6)$$

Table 1
Inorganic eutectic salt mixtures with potential for use as PCMs for moderate to high temperature heat storage applications (Demirbas, 2006; Zalba, Mari'n, Cabeza, & Mehling, 2003).

Compound	Melting temperature (K)	Heat of fusion (kJ/kg)	Thermal conductivity (W/(m K))	Density (kg/m ³)
68.1% KCl ₂ + 31.9% ZnCl ₂	508	198	n.a.	2480
NaNO ₃	580	199	0.5	2257
KNO ₃	606	266	0.5	2110
KOH	653	150	0.5	2044
38.5% MgCl ₂ + 61.5% NaCl	708	328	n.a.	2160
11.8% NaF + 54.3% KF + 26.6% LiF + 7.3% MgF ₂	722	n.a.	n.a.	2160
35.1% LiF + 38.4% NaF + 26.5% CaF ₂	888	n.a.	n.a.	2225
32.5% LiF + 50.5% NaF + 17.0% MgF ₂	905	n.a.	n.a.	2105
51.8% NaF + 34.0% CaF ₂ + 14.2% MgF ₂	918	n.a.	n.a.	2370
48.1 LiF + 51.9% NaF	925	n.a.	n.a.	1930
MgCl ₂	987	452	n.a.	2140

%; percentage in weight; n.a.: not available.

Table 2

PCM eutectic solutions with potential for use in high-grade cold storage applications (Medrano, Gil, Martorell, Potau, & Cabeza, 2010).

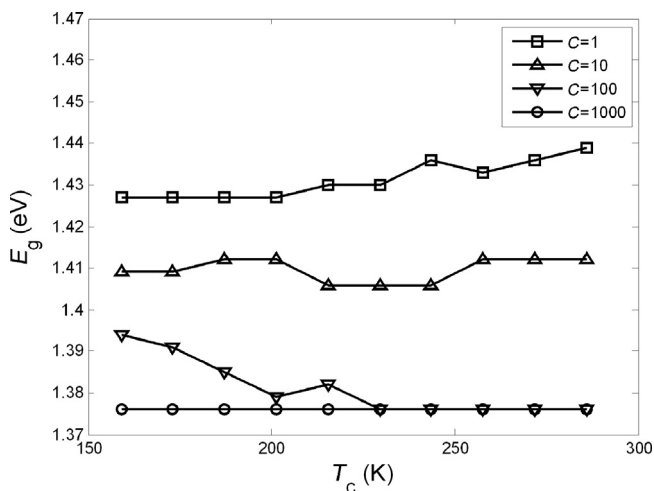
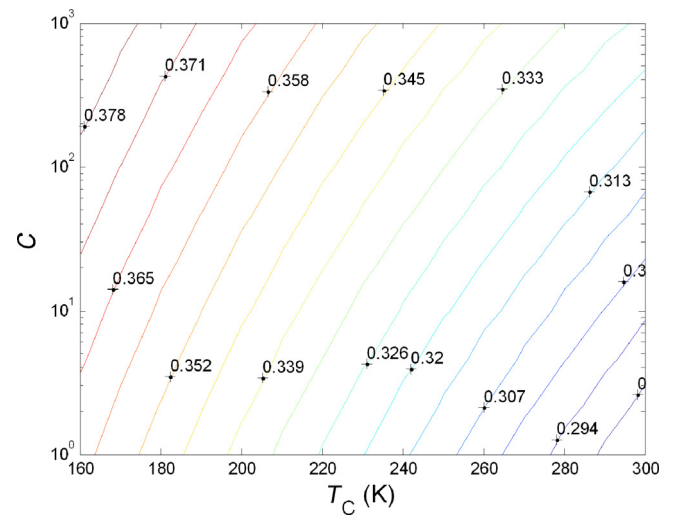
PCM type	Phase change temperature (K)	Heat capacity (kJ/kg)	Thermal conductivity (W/(m K))	Density (kg/m ³)
E-46	227	240	0.54	1405
E-50	223	218	0.56	1325
E-60	213	172	0.44	1180
E-62	211	180	0.58	1125
E-75	198	102	0.17	902
E-78	195	115	0.14	880
E-90	183	90	0.14	786
E-114	159	107	0.17	782

Here, α_{PV} and α_{TE} are the operational efficiencies of the PV cell and the TE generator, respectively, indicating the ratios of the net practical electric power output of the devices to the corresponding ideal outputs. Considering that the best efficiencies for all well-developed PV cells and TE generators are around 0.8, it is reasonable to set the two operational efficiencies as 0.75 in the calculations (Vorobiev et al., 2006). Note also that the operational efficiency includes the heat losses in the heat storage process for the TE generators. In the equation, η_{IA} is the incomplete absorption efficiency, which denotes the split from the solar radiation to the generator at moderate to high temperature thermal energies. From the descriptions given in Section 2, we see that the total conversion efficiency can be expressed as follows:

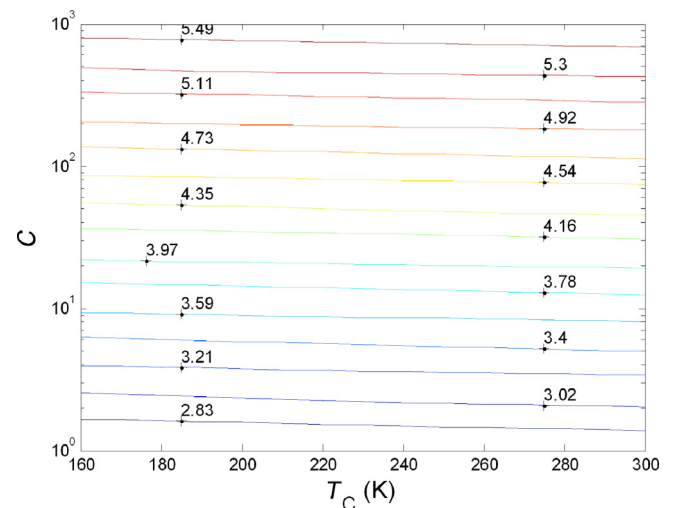
$$\eta_{total} = f(E_g, C, ZT, T_h, T_c). \quad (7)$$

An optimal band gap E_g exists that leads to the best system performance level, depending on the PV operating temperature T_c and the concentration ratio C . For given T_c and C , the optimal band gap can be found by maximizing Eq. (7). This process has been coded in Matlab environment using genetic algorithm. The simulation result is shown in Fig. 7, from which we can see that the optimal band gap varies slightly with changes in operating temperature. In other words, a cell with a suitable band gap could provide good performance over a wide operating temperature range.

Obviously, the optimal band gap decreases with increasing concentration ratio. Using the optimal band gap obtaining in Fig. 7, the total efficiencies for given operating temperature and concentration ratio are shown in Fig. 8, with the assumptions that $ZT = 2$ and $T_h = 600$ K. It reveals that a higher concentration ratio produces a higher total efficiency. It also shows that a tenfold increase in the concentration ratio contributes an increase of approximately 0.8% to the total efficiency. In terms of the operating temperature, this is

**Fig. 7.** Optimum energy band gap for the PV under different operating temperatures and concentration ratios.**Fig. 8.** The contour demonstrating dependence of the total efficiency on the operating temperature T_c and the concentration ratio C for $T_h = 600$ K and $ZT = 2$.

equivalent to a decrease of 14 K. By deeply decreasing the operating temperature from the ambient temperature down to approximately 160 K, the total efficiency improves by about 8%, regardless of the concentration ratio. This corresponds to an increase of nearly 30% in the output power. However, increasing the concentration ratio raises the cooling power load per unit area linearly on the PV surface, as shown in Fig. 9. For this reason, the concentration

**Fig. 9.** The contour demonstrating dependence of the cooling power per unit area of the PV surface Q (W/m²) on the concentration ratio C and the operating temperature T_c .

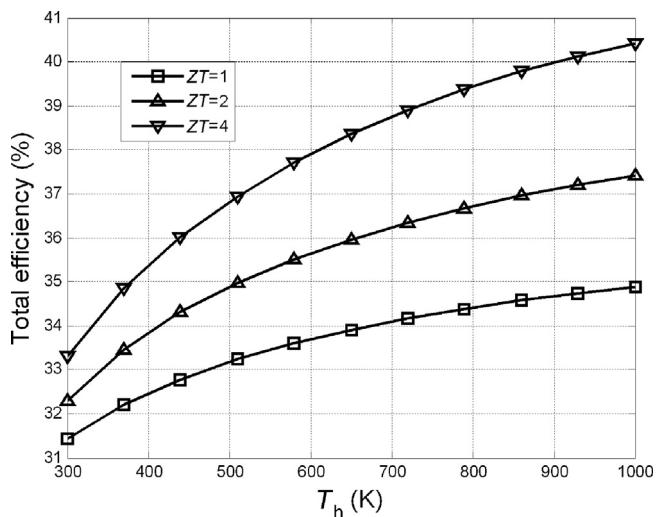


Fig. 10. The dependence of total efficiency on the hot side temperature T_h and dimensionless thermoelectric coefficient ZT , with $C = 100$ and $T_c = 200$ K.

ratio must be kept below 100 in practical applications (Meneses-Rodríguez, Horley, González-Hernández, Vorobiev, & Gorley, 2005).

The dependence of total efficiency on the hot side temperature T_h and dimensionless thermoelectric coefficient ZT of the TE generator is shown in Fig. 10. It shows that the total efficiency has increased, but the rate of this increase declines with increasing hot side temperature. In contrast, doubling the value of the dimensionless thermoelectric coefficient ZT yields an improvement of more than 2% in the total efficiency. From Fig. 10, we can also see that at peak times, the total efficiency of the integrated system is around 31–34% based on currently available TE materials ($ZT = 1$). This indicates that the proposed system can deliver more than double the power of current PV cells alone. Although part of the power output comes from the stored thermal energy (both cold and heat), this indicates that the hybrid system is potentially capable of delivering power to end-users at the desired times and rates.

4. Conclusions

This paper proposes conceptually a hybrid PV–TE power system that is integrated with a high-grade heat and cold energy storage facility for efficient solar energy harvesting. The concept of supercooling of the PV cell has been introduced to increase the output power at peak times. Calculations based on the basic principles show that a 30% improvement in the output power could be achieved by adding a high-grade cold energy storage system under reasonable working conditions. In addition, a suitable single band-gap PV cell could produce good performances at both peak and off-peak times because it is independent of the operating temperature. Increases in the concentration ratio, the hot side temperature and the dimensionless thermoelectric coefficient also contribute to an increased total efficiency, despite the other associated difficulties.

The simple structure and the absence of moving parts mean that the proposed system could potentially be used as a domestic power generator that supplies not only electricity but also heat and cold throughout the year.

Acknowledgements

This work has been supported by the Focused Deployment Project of the Chinese Academy of Sciences (KGZD-EW-302-1), the

Key Technologies R&D Program of China (grant no. 2012BAA03B03) and by a UK EPSRC grant under EP/K002252/1.

References

- Beard, M. C., & Ellingson, R. J. (2008). Multiple exciton generation in semiconductor nanocrystals: Toward efficient solar energy conversion. *Laser & Photonics Reviews*, 2, 377–399.
- Chen, J. (1996). Thermodynamic analysis of a solar-driven thermoelectric generator. *Journal of Applied Physics*, 79(5), 2717–2721.
- Crabtree, G. W., & Lewis, N. S. (2007). Solar energy conversion. *Physics Today*, 60, 37–42.
- Demirbas, M. F. (2006). Thermal energy storage and phase change materials: An overview. *Energy Sources, Part B*, 1(1), 85–95.
- Hanna, M. C., & Nozik, A. J. (2006). Solar conversion efficiency of photovoltaic and photoelectrolysis cells with carrier multiplication absorbers. *Journal of Applied Physics*, 100(7), 074510.
- Henry, C. H. (1980). Limiting efficiencies of ideal single and multiple energy gap terrestrial solar cells. *Journal of Applied Physics*, 51(8), 4494–4500.
- Imenes, A. G., & Mills, D. R. (2004). Spectral beam splitting technology for increased conversion efficiency in solar concentrating systems: A review. *Solar Energy Materials and Solar Cells*, 84(1–4), 19–69.
- Kovalenko, M. V., Spokoyny, B., Lee, J.-S., Scheele, M., Weber, A., Perera, S., et al. (2010). Semiconductor nanocrystals functionalized with antimony telluride zintl ions for nanostructured thermoelectrics. *Journal of the American Chemical Society*, 132, 6686–6695.
- Kraemer, D., Hu, L., Muto, A., Chen, X., Chen, G., & Chiesa, M. (2008). Photovoltaic-thermoelectric hybrid systems: A general optimization methodology. *Applied Physics Letters*, 92(24), 243503.
- Li, C. H., Zhu, X. J., Cao, G. Y., Sui, S., & Hu, M. R. (2009). Dynamic modeling and sizing optimization of stand-alone photovoltaic power systems using hybrid energy storage technology. *Renewable Energy*, 34(3), 815–826.
- Li, Y., Chen, H., & Ding, Y. (2010). Fundamentals and applications of cryogen as a thermal energy carrier: A critical assessment. *International Journal of Thermal Sciences*, 49(6), 941–949.
- Li, Y., Jin, Y., Chen, H., Tan, C., & Ding, Y. (2011). An integrated system for thermal power generation, electrical energy storage and CO₂ capture. *International Journal of Energy Research*, 35, 1158–1167.
- Luque, A., & Martí, A. (2001). A metallic intermediate band high efficiency solar cell. *Progress in Photovoltaics: Research and Applications*, 9(2), 73–86.
- Maclay, J. D., Brouwer, J., & Samuelson, G. S. (2007). Dynamic modeling of hybrid energy storage systems coupled to photovoltaic generation in residential applications. *Journal of Power Sources*, 163(2), 916–925.
- Medrano, M., Gil, A., Martorell, I., Potau, X., & Cabeza, L. F. (2010). State of the art on high-temperature thermal energy storage for power generation. Part 2—Case studies. *Renewable & Sustainable Energy Reviews*, 14(1), 56–72.
- Meneses-Rodríguez, D., Horley, P. P., González-Hernández, J., Vorobiev, Y. V., & Gorley, P. N. (2005). Photovoltaic solar cells performance at elevated temperatures. *Solar Energy*, 78(2), 243–250.
- Miljkovic, N., & Wang, E. N. (2011). Modeling and optimization of hybrid solar thermoelectric systems with thermosyphons. *Solar Energy*, 85(11), 2843–2855.
- Nolas, G. S., Sharp, J., & Goldsmid, J. (2001). *Thermoelectrics, basic principles and new materials developments*. Berlin: Springer-Verlag.
- Nozik, A. J. (2001). Spectroscopy and hot electron relaxation dynamics in semiconductor quantum wells and quantum dots. *Annual Review of Physical Chemistry*, 52, 193–231.
- Odeh, S., & Behnia, M. (2009). Improving photovoltaic module efficiency using water cooling. *Heat Transfer Engineering*, 30, 499–505.
- Omer, S. A., & Infield, D. G. (1998). Design optimization of thermoelectric devices for solar power generation. *Solar Energy Materials and Solar Cells*, 53, 67–82.
- Rockendorf, G., Sillmann, R., Podlowski, L., & Litzenburger, B. (1999). PV-hybrid and thermoelectric collectors. *Solar Energy*, 67, 227–237.
- Rowe, D. M. (1995). *CRC handbook of thermoelectrics*. Boca Raton: CRC Press.
- Royne, A., Dey, C. J., & Mills, D. R. (2005). Cooling of photovoltaic cells under concentrated illumination: A critical review. *Solar Energy Materials and Solar Cells*, 86(4), 451–483.
- Scheele, M., Oeschler, N., Meier, K., Kornowski, A., Klinke, C., & Weller, H. (2009). Synthesis and thermoelectric characterization of Bi₂Te₃ nanoparticles. *Advanced Functional Materials*, 19, 3476–3483.
- Thiruganasambandam, M., Iniyar, S., & Goic, R. (2010). A review of solar thermal technologies. *Renewable & Sustainable Energy Reviews*, 14(1), 312–322.
- Tritt, T. M., Böttner, H., & Chen, L. (2008). Thermoelectrics: Direct solar thermal energy conversion. *MRS Bulletin*, 33, 366–368.
- Van Sark, W. G. J. H. M. (2011). Feasibility of photovoltaic–Thermoelectric hybrid modules. *Applied Energy*, 88, 2785–2790.
- Vorobiev, Y., González-Hernández, J., Vorobiev, P., & Bulat, L. (2006). Thermal-photovoltaic solar hybrid system for efficient solar energy conversion. *Solar Energy*, 80(2), 170–176.
- Yang, D., & Yin, H. (2011). Energy conversion efficiency of a novel hybrid solar system for photovoltaic, thermoelectric, and heat utilization. *IEEE Transactions on Energy Conversion*, 26(2), 662–670.
- Zalba, B., Marín, J. M., Cabeza, L. F., & Mehling, H. (2003). Review on thermal energy storage with phase change: Materials, heat transfer analysis and applications. *Applied Thermal Engineering*, 23(3), 251–283.